

Tiling Phosphorene

Jie Guan,^{†,‡} Zhen Zhu,^{†,‡} and David Tománek^{*,†}

Physics and Astronomy Department, Michigan State University, East Lansing, Michigan 48824, USA

E-mail: tomanek@pa.msu.edu

Abstract

We present a scheme to categorize the structure of different layered phosphorene allotropes by mapping their non-planar atomic structure onto a two-color 2D triangular tiling pattern. In the buckled structure of a phosphorene monolayer, we assign atoms in “top” positions to dark tiles and atoms in “bottom” positions to light tiles. Optimum sp^3 bonding is maintained throughout the structure when each triangular tile is surrounded by the same number N of like-colored tiles, with $0 \leq N \leq 2$. Our *ab initio* density functional calculations indicate that both the relative stability and electronic properties depend primarily on the structural index N . The proposed mapping approach may also be applied to phosphorene structures with non-hexagonal rings and 2D quasicrystals with no translational symmetry, which we predict to be nearly as stable as the hexagonal network.

Keywords: black phosphorus, phosphorene, DFT, *ab initio*, structure, band structure, stability

Phosphorene, a monolayer of black phosphorus, is emerging as a viable contender in the field of two-dimensional (2D) electronic materials.^{1–3} In comparison to the widely discussed semi-metallic

graphene, phosphorene displays a significant band gap while still maintaining a high carrier mobility.^{3–6} The flexible structure of semiconducting phosphorene^{7,8} is advantageous in applications including gas sensing,⁹ thermoelectrics,¹⁰ and Li-ion batteries.¹⁰ Unlike flat sp^2 -bonded graphene monolayers, the structure of sp^3 -bonded phosphorene is buckled. There is a large number of sp^3 -bonded layered phosphorene structures, including blue-P, γ -P, and δ -P,^{11,12} which are nearly as stable as the related black phosphorene structure but exhibit very different electronic properties. We believe that the above list of stable phosphorene structures is still incomplete, giving rise to an unprecedented richness in terms of polymorphs and their electronic structure.

Here we introduce a scheme to categorize the structure of different layered phosphorene allotropes by mapping the non-planar 3D structure of three-fold coordinated P atoms onto a two-color 2D triangular tiling pattern. In the buckled structure of a phosphorene monolayer, we assign atoms in “top” positions to dark tiles and atoms in “bottom” positions to light tiles. Optimum sp^3 bonding is maintained throughout the structure when each triangular tile is surrounded by the same number N of like-colored tiles, with $0 \leq N \leq 2$. Our *ab initio* density functional calculations indicate that both the relative stability and electronic properties depend primarily on the structural index N . Common characteristics of allotropes with identical N suggest the usefulness of the structural index for categorization. The proposed mapping approach may also be applied to phosphorene structures with non-hexagonal rings, counterparts of

*To whom correspondence should be addressed

[†]Physics and Astronomy Department, Michigan State University, East Lansing, Michigan 48824, USA

[‡]These authors contributed equally to this work.

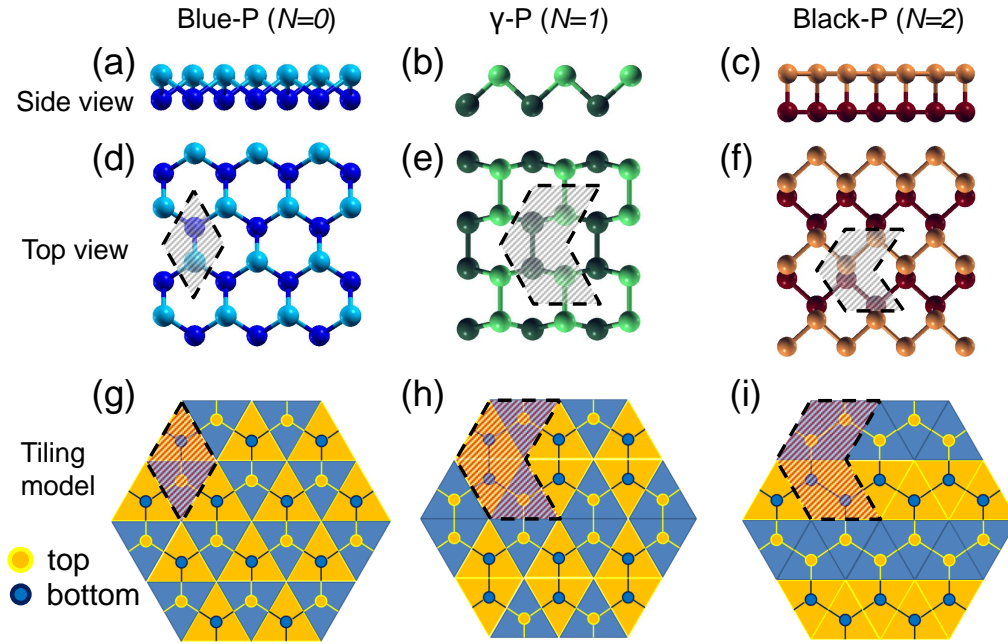


Figure 1: (Color online) Atomic structure of different phosphorene allotropes in (a-c) side view, (d-f) top view, and (g-i) in a tiling model representation. Blue-P (a,d,g), γ -P (b,e,h), and black-P (c,f,i) can be distinguished by the structural index N . Primitive unit cells are emphasized by shading and delimited by black dashed lines in (d-i). Atoms at the top and bottom of the layer, as well as the corresponding tiles, are distinguished by color.

planar haeckelite,^{13,14} to point and line defects,¹⁵ and to 2D quasicrystals with no translational symmetry, which we predict to be nearly as stable as the hexagonal network.

Results and discussion

The non-planar atomic structure of selected sp^3 -bonded phosphorene allotropes is depicted in side and top view in Fig. 1(a-f). We find it convenient to map the 3D structure of a phosphorene monolayer with threefold coordinated atoms onto a 2D tiling pattern by assigning a triangular tile to each atom, as shown in Fig. 1(g-i). There is a one-to-one correspondence between structures and tiling patterns, so that different structures can be distinguished by different tiling patterns. Dark-colored tiles are associated with atoms at the top and light-colored tiles with atoms at the bottom of the layer. Since each atom has 3 neighbors, each triangular tile is surrounded by 3 neighboring tiles, N of which have the same color. It is obvious that $0 \leq N \leq 2$ provides the atom associated with the central tile with a tetrahedral neighbor co-

ordination associated with the favorable sp^3 bonding. In our tiling model, $N = 3$ would represent the planar structure of an energetically unfavorable sp^2 -bonded lattice that, according to our findings, would spontaneously convert to a non-planar sp^3 -bonded allotrope.

As we will show in the following, different allotropes with $N = 0$, $N = 1$ and $N = 2$ share similar characteristics. Therefore, the structural index N is useful for primary categorization of the allotropes. In each structure depicted in Fig. 1, N maintains an identical value throughout the lattice, keeping the favorable sp^3 bonding at all sites. We believe that this is the underlying reason for our finding that these structures are nearly equally stable.^{11,12}

In the first category characterized by $N = 0$, all neighbors of a given atom have the same, but different height within the layer, as seen in Figs. 1(a) and 1(d). This translates into a tiling pattern, where all adjacent tiles have a different color, as seen in Fig. 1(g). There is only one structural realization within the $N = 0$ category, namely the blue-P allotrope.

In the second category characterized by $N = 1$, each atom has one like neighbor at the same height

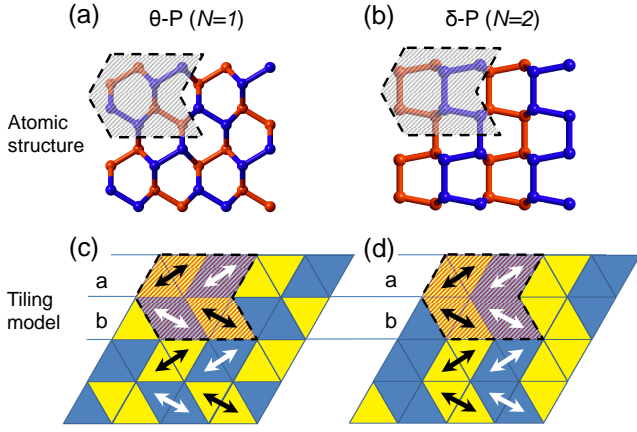


Figure 2: (Color online) Atomic structure of $N = 1$ and $N = 2$ phosphorene allotropes in top view (a-b) and the corresponding tiling model representation (c-d). The $N = 1$ θ -P allotrope in (a,c) and the $N = 2$ allotrope in (b,d) are structurally different from the allotropes with the same N in Fig. 1. Primitive unit cells are emphasized by shading and delimited by black dashed lines. Atoms at the top and bottom of the layer, as well as the corresponding tiles, are distinguished by color. The two different orientations of bonds between like atoms, indicated by the double arrows as guides to the eye, are denoted by “ a ” and “ b ”.

and two unlike neighbors at a different height within the layer, as seen in Figs. 1(b) and 1(e). Besides the γ -P structure in Fig. 1(b) and 1(e), there is a θ -P allotrope, depicted Fig. 2(a), with the same structural index $N = 1$. The tiling patterns of γ -P and θ -P, shown in Figs. 1(h) and 2(c), are characterized by a diamond harlequin pattern. Each diamond, formed of two adjacent like-colored triangles, is surrounded by unlike-colored diamonds. As a guide to the eye, we indicate the orientation of the diamonds, same as the direction of the atomic bonds, by the double arrows in Fig. 2(c). The shape of the primitive unit cells shown in Figs. 1 and 2 is chosen to see more easily the correspondence between the atomic structure and the tiling pattern. The primitive unit cell of γ -P contains 4 atoms according to Fig. 1(h) and that of θ -P contains 8 atoms, as seen in Fig. 2(c). As indicated in Fig. 2(c), the orientation of diamonds in a row may be distinguished by the letters “ a ” or “ b ”. Whereas the perfect γ -P structure in Fig. 1(h) could be characterized by the sequence “ $aaaa\dots$ ” and the structure of θ -P by the sequence “ $abab\dots$ ”, an

infinite number of different sequences including “ $abaa\dots$ ” would result in an infinite number of $N = 1$ phosphorene structures.

The most stable and best-known phosphorene allotrope is black-P, depicted in Fig. 1(c) and 1(f). Each atom in this structure has two like neighbors at the same height and one unlike neighbor at a different height, yielding a structural index $N = 2$. The tiling model of this structure type, shown in Fig. 1(i), contains contiguous arrays of like-colored diamonds. These arrays may be either straight, as in Fig. 1(i) for black-P, or not straight, as in Fig. 2(d) for the structurally different δ -P allotrope with the atomic structure shown in Fig. 2(b). Describing diamond orientation by letters “ a ” and “ b ” as in the case of $N = 1$, we may characterize black-P in Fig. 1(i) by the sequence “ $aaaa\dots$ ” and δ -P in Fig. 2(d) by the sequence “ $abab\dots$ ”. As in the case of $N = 1$, an infinite number of different sequences including “ $abaa\dots$ ” would result in an infinite number of $N = 2$ phosphorene structures.

The structural similarity and energetic near-degeneracy of $N = 2$ and $N = 1$ structures stems from the fact that a structural change from $N = 2$ to $N = 1$ involves only a horizontal shift of every other row, indicated by the horizontal lines in Figs. 2(c) and 2(d), by one tile. It is even possible to generate structural domains with different values of N . The energy cost of domain wall boundaries may be extremely low¹² if optimum sp^3 bonding is maintained at the boundaries.

As mentioned above, there is only one allotrope with $N = 0$, but infinitely many structures with $N = 1$ and $N = 2$. Of these, we identified and optimized all lattices with up to 28 atoms per primitive unit cell and selected other structures with up to 32 atoms per unit cell. For each lattice, we identified the relative stability ΔE with respect to the most stable black phosphorene allotrope on a per-atom basis and plotted the values in Fig. 3(a).

The electronic band structure of systems with large unit cells is very dense and hard to interpret in comparison to that of the allotropes discussed in Figs. 1 and 2, which is reproduced in the Supporting Information.¹⁶ For each of these structures, though, we identified the value E_g of the fundamental band gap and provide the results in Fig. 3(b).

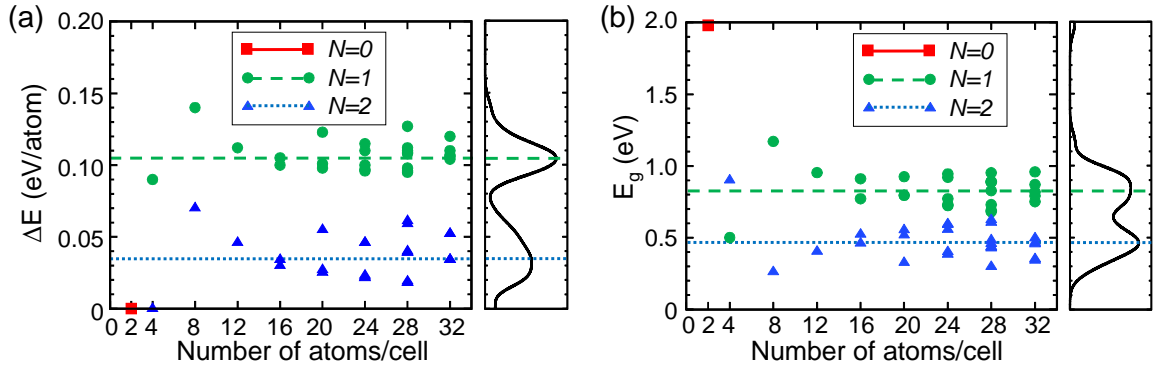


Figure 3: (Color online) (a) Relative stability ΔE of different phosphorene allotropes with respect to black phosphorus and (b) their fundamental band gap E_g . The distribution of the ΔE and E_g values, provided in the right panels of the subfigures, indicates presence of three distinguishable groups that may be linked to the different values of the structural index N . The dashed and dotted lines are guides to the eye.

We find that neither ΔE nor E_g display a general dependence on the size of the unit cell. We found all structures to be relatively stable. The small values $\Delta E < 0.15$ eV/atom indicate a likely coexistence of different allotropes that would form under nonequilibrium conditions. All band gap values, which are typically underestimated in DFT-PBE calculations,^{17,18} occur in the range between 0.3 eV and 2.0 eV, similar to the allotropes discussed in Figs. 1 and 2. Rather surprisingly, the distribution of ΔE and E_g values, shown in the right panels of the sub-figures Fig. 3(a) and 3(b), exhibits three peaks that can be associated with the structural index N , with a rather narrow variance caused by the differences between the allotrope structures. We find the energetically near-degenerate blue phosphorene ($N = 0$ with 2 atoms per unit cell) and black phosphorene ($N = 2$ with 4 atoms per unit cell) structures to be the most stable, followed by other $N = 2$ structures with more than 4 atoms per unit cell. We found $N = 1$ structures to be the least stable of all. Similarly, the $N = 0$ blue phosphorene allotrope has the largest band gap, $N = 2$ allotropes have the smallest band gap, and $N = 1$ allotropes lie in between.

The higher stability of $N = 2$ phosphorene structures in comparison to $N = 1$ allotropes indicates an energetic preference for phosphorus atoms forming zigzag chains at the same height rather than forming isolated dimers. Among the $N = 2$ structures, δ -P is the least stable, with $\Delta E \approx 0.07$ eV/atom. All the other $N = 2$ structures fall in-between δ -P and black phosphorus in

terms of stability. This finding is easy to understand, since all these structures are combination of black phosphorus and δ -P.

For both $N = 2$ and $N = 1$ allotropes, we find structures with the same orientation of diamonds in the tiling pattern to be more stable. The γ -P structure, with all diamonds aligned in the same direction in the tiling pattern, is the most stable $N = 1$ phosphorene allotrope, but still less stable by 0.09 eV/atom than the $N = 2$ black phosphorene. At the other extreme of the relative stability range, θ -P with disordered diamond orientations in the tiling pattern is the least stable $N = 1$ allotrope, being 0.14 eV/atom less stable than black phosphorene. In analogy to what we concluded for $N = 2$ structures, all $N = 1$ phosphorene allotropes can be viewed as a combination of γ -P and θ -P, with their stability in-between the above limiting values.

As mentioned above, also the distribution of E_g values, shown in the right panel of Fig. 3(b), indicates three distinct groups that can be associated with the structural index N . The largest band gap value of 2.0 eV in the only $N = 0$ structure, blue phosphorene, is well separated from the band gap distribution of $N = 1$ and $N = 2$ structures that form a double-hump shape. We note that the two peaks in the band gap distribution of $N = 1$ and $N = 2$ allotropes are not as well separated as the two peaks in the stability distribution in Fig. 3(a), so the trends in the band gap value are not as clear as trends in the relative stability. In systems with large unit cells, band gaps of $N = 1$ structures

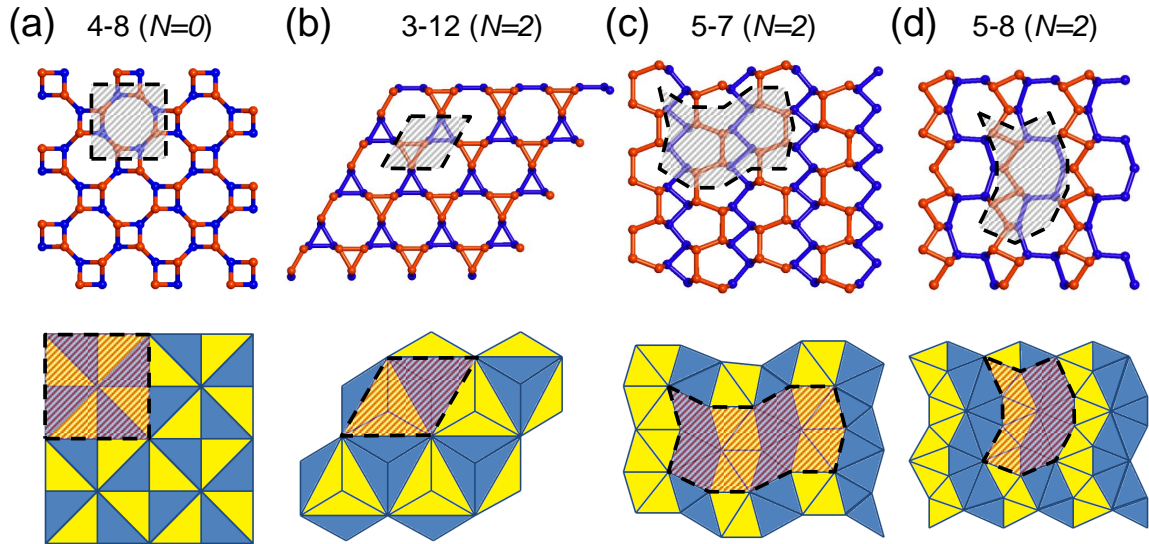


Figure 4: (Color online) Equilibrium structures (top) and corresponding tiling patterns (bottom) of 2D phosphorene with (a) 4-8, (b) 3-12, (c) 5-7, and (d) 5-8 membered rings. The color of the atoms and corresponding tiles distinguishes positions at the top and the bottom of the layer.

are grouped around 0.8 eV, whereas band gaps of $N = 2$ structures are grouped around 0.5 eV. The largest spread in E_g values is in systems with very small unit cells. Among $N = 1$ allotropes, we find the smallest value $E_g \approx 0.5$ eV in the structure with 4 atoms/unit cell (γ -P) and the largest value $E_g \approx 1.2$ eV in the structure with 8 atoms/unit cell (θ -P). Band gap values of other $N = 1$ structures range between these two values. $N = 2$ structures have generally the lowest band gap values of the three groups. Among $N = 2$ systems, we find the largest value $E_g \approx 0.9$ eV in the structure with 4 atoms/unit cell (black phosphorene) and $E_g \approx 0.3$ eV in a system with 8 atoms/unit cell, the smallest gap value among several metastable structures of δ -P. Band gap values of other $N = 2$ structures range between these two values. As discussed earlier,^{11,12} our PBE-based band gap values are generally underestimated. More precise quasiparticle calculations beyond DFT, including the GW formalism, indicate that the band gap values should be about 1 eV larger than the PBE values presented here.^{11,19}

As the unit cell size of $N = 1$ and $N = 2$ structures grows infinitely large, we gradually approach amorphous phosphorene. Assuming that our findings in Fig. 3 are universal and not limited to the finite sizes addressed by our study, we conclude that the stability and the fundamental band gap of

such amorphous structures should also be found in the range suggested by their structural index N .

The one-to-one mapping between 3D structures of periodic systems and 2D tiling patterns is not limited to a honeycomb lattice with 6-membered rings, but can equally well be applied to lattices with 3-, 4-, 5-, 7-, 8- and 12-membered rings found in planar haeckelites.^{13,14} The corresponding geometries and tiling patterns are shown in Fig. 4. Among these structures, 4-8 phosphorene has the highest symmetry, a relatively small unit cell with the shape of a square and a tiling pattern composed of right triangles. Besides the $N = 0$ structure depicted in Fig. 4(a), we can identify allotropes with 4-8 rings with structural indices $N = 1$ and $N = 2$. Other allotropes with 3-12, 5-7 and 5-8 rings, shown in Figs. 4(b-d), may not exist in all the variants of the structural index N due to their lower symmetry. For example, the allotrope with 5-7 rings does not have a structure with $N = 0$.

We find structures with non-hexagonal rings to be generally less stable than the most stable black phosphorene, but the energy differences $\Delta E < 0.2$ eV/atom are very small. Consequently, we expect that such structures should coexist with black phosphorene as either pure phases, or as local defects at domain wall boundaries, or as finite-size domains in the host layer. We find all phosphorene

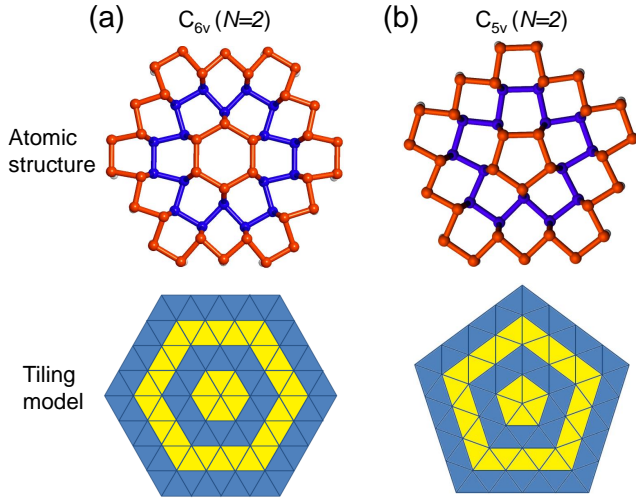


Figure 5: (Color online) Equilibrium structures (top panels) and corresponding tiling patterns (bottom panels) of phosphorene structures with (a) a C_{6v} and (b) a C_{5v} symmetry. Edges of the finite-size flakes are terminated by hydrogen atoms, colored in white. The color of the phosphorus atoms and the corresponding tiles distinguishes positions at the top or the bottom of the layer.

allotropes with non-hexagonal rings to be semiconducting, with the band gap determined primarily by the structural index N .

Phosphorene may also form aperiodic structures with no translational symmetry. Examples of such systems with only rotational symmetry are shown in Fig. 5. Fig. 5(a) depicts a phosphorene structure of type $N = 2$ with a C_{6v} point group symmetry and the corresponding tiling pattern. In this structure, arrays of neighboring atoms form an alternating circular pattern about the center that can cover an infinite plane. The analogous $N = 2$ structure with C_{5v} symmetry is depicted in Fig. 5(b), and analogous structures with C_{nv} symmetry could be imagined as well. To judge the stability of these aperiodic structures, we optimized finite-size flakes that were terminated by hydrogen atoms at the exposed edge. We found these structures to be semiconducting and as stable as the periodic structures discussed in Fig. 3(a), with $\Delta E = 0.07$ eV/atom for the C_{6v} and $\Delta E = 0.04$ eV/atom for the C_{5v} structure falling into range expected for $N = 2$.

These findings indicate that our classification scheme and tiling model is useful to characterize monolayers of three-fold coordinated, sp^3 -hybridized phosphorus atoms arranged in periodic

or aperiodic patterns. Due to structural similarities between layered structures of group-V elements, we believe that our findings regarding relative stability, electronic structure and fundamental band gap will likely also apply to other systems including monolayers of arsenic, antimony and bismuth.

Since the cohesive energy differences are rather small, we must consider the possibility that the stability ranking of the different allotropes at $T = 0$ and related properties²⁰ may depend on the DFT functional. We have compared PBE results for the relative stability of the different allotropes with LDA results and found the maximum difference in the relative stabilities of the different allotropes to be 0.02 eV/atom, which does not change the energy ranking of the allotropes.

Since phosphorene structures will likely be synthesized at nonzero temperatures, the relative abundance of different allotropes will depend on their free energy at that temperature. Consequently, our total energy results for stability differences at $T = 0$ need to be corrected by also addressing differences in entropy at $T > 0$. Even though the decrease in free energy with increasing temperature should be similar in the different allotropes due to their similar vibration spectra,^{11,12,16} minute differences in vibrational entropy may become important in view of the small differences between stabilities of the allotropes at $T = 0$, and could eventually change the free energy ranking at high temperatures.

In conclusion, we have introduced a scheme to categorize the structure of different layered phosphorene allotropes by mapping the non-planar 3D structure of three-fold coordinated P atoms onto a two-color 2D triangular tiling pattern. In the buckled structure of a phosphorene monolayer, we assign atoms in “top” positions to dark tiles and atoms in “bottom” positions to light tiles. We found that optimum sp^3 bonding is maintained throughout the structure when each triangular tile is surrounded by the same number N of like-colored tiles, with $0 \leq N \leq 2$. Our *ab initio* density functional calculations indicate that both the relative stability and electronic properties depend primarily on the structural index N . Common characteristics of allotropes with identical N suggest the usefulness of the structural index for categorization. The proposed mapping approach may also

be applied to phosphorene structures with non-hexagonal rings and to 2D quasicrystals with no translational symmetry, which we predict to be nearly as stable as the hexagonal network.

Methods

Our computational approach to gain insight into the equilibrium structure, stability and electronic properties of various phosphorene structures is based on *ab initio* density functional theory (DFT) as implemented in the SIESTA.¹⁷ We used periodic boundary conditions throughout the study. We used the Perdew-Burke-Ernzerhof (PBE)¹⁸ exchange-correlation functional, norm-conserving Troullier-Martins pseudopotentials,²¹ and a double- ζ basis including polarization orbitals. Selected PBE results were compared to results based on the Local Density Approximation (LDA).^{22,23} The reciprocal space was sampled by a fine grid²⁴ of $8 \times 8 \times 1$ k -points in the Brillouin zone of the primitive unit cell. We used a mesh cutoff energy of 180 Ry to determine the self-consistent charge density, which provided us with a precision in total energy of ≤ 2 meV/atom. All geometries have been optimized by SIESTA using the conjugate gradient method,²⁵ until none of the residual Hellmann-Feynman forces exceeded 10^{-2} eV/Å.

Acknowledgement We thank Luke Shulenburg for useful discussions. This study was supported by the National Science Foundation Cooperative Agreement #EEC-0832785, titled “NSEC: Center for High-rate Nanomanufacturing”. Computational resources have been provided by the Michigan State University High Performance Computing Center. shown in this document.

Supporting Information Available: Electronic band structure of the phosphorene allotropes discussed in Figs. 1 and 2 and phonon band structure of θ -P. This material is available free of charge via the Internet at <http://pubs.acs.org/>.

References

1. Narita, S.; Akahama, Y.; Tsukiyama, Y.; Muro, K.; Mori, S.; Endo, S.; Taniguchi, M.; Seki, M.; Suga, S.; Mikuni, A. *et al.* Electrical and Optical Properties of Black Phosphorus Single Crystals. *Physica B+C* **1983**, *117&118*, 422–424.
2. Maruyama, Y.; Suzuki, S.; Kobayashi, K.; Tanuma, S. Synthesis and Some Properties of Black Phosphorus Single Crystals. *Physica B+C* **1981**, *105*, 99–102.
3. Liu, H.; Neal, A. T.; Zhu, Z.; Luo, Z.; Xu, X.; Tomanek, D.; Ye, P. D. Phosphorene: An Unexplored 2D Semiconductor with a High Hole Mobility. *ACS Nano* **2014**, *8*, 4033–4041.
4. Li, L.; Yu, Y.; Ye, G. J.; Ge, Q.; Ou, X.; Wu, H.; Feng, D.; Chen, X. H.; Zhang, Y. Black phosphorus field-effect transistors. *Nature Nanotech.* **2014**, *9*, 372–377.
5. Koenig, S. P.; Doganov, R. A.; Schmidt, H.; Castro Neto, A. H.; Özyilmaz, B. Electric Field Effect in Ultrathin Black Phosphorus. *Appl. Phys. Lett.* **2014**, *104*, 103106.
6. Xia, F.; Wang, H.; Jia, Y. Rediscovering Black Phosphorus: A Unique Anisotropic 2D Material for Optoelectronics and Electronics. *Nature Commun.* **2014**, *5*, 4458.
7. Fei, R.; Yang, L. Strain-Engineering the Anisotropic Electrical Conductance of Few-Layer Black Phosphorus. *Nano Lett.* **2014**, *14*, 2884–2889.
8. Rodin, A. S.; Carvalho, A.; Castro Neto, A. H. Strain-Induced Gap Modification in Black Phosphorus. *Phys. Rev. Lett.* **2014**, *112*, 176801.
9. Kou, L.; Frauenheim, T.; Chen, C. Phosphorene as a Superior Gas Sensor: Selective Adsorption and Distinct I-V Response. *J. Phys. Chem. Lett.* **2014**, *5*, 2675–2681.
10. Fei, R.; Faghaninia, A.; Soklaski, R.; Yan, J.-A.; Lo, C.; Yang, L. Enhanced Thermoelectric

- Efficiency via Orthogonal Electrical and Thermal Conductances in Phosphorene. *Nano Lett.* **2014**, *14*, 6393–6399.
11. Zhu, Z.; Tománek, D. Semiconducting Layered Blue Phosphorus: A Computational Study. *Phys. Rev. Lett.* **2014**, *112*, 176802.
 12. Guan, J.; Zhu, Z.; Tománek, D. Phase Coexistence and Metal-Insulator Transition in Few-Layer Phosphorene: A Computational Study. *Phys. Rev. Lett.* **2014**, *113*, 046804.
 13. Fthenakis, Z. G.; Zhu, Z.; Tománek, D. Effect of Structural Defects on the Thermal Conductivity of Graphene: From Point to Line Defects to Haeckelites. *Phys. Rev. B* **2014**, *89*, 125421.
 14. Terrones, H.; Terrones, M.; Hernández, E.; Grobert, N.; Charlier, J.-C.; Ajayan, P. M. New Metallic Allotropes of Planar and Tubular Carbon. *Phys. Rev. Lett.* **2000**, *84*, 1716–1719.
 15. Liu, Y.; Xu, F.; Zhang, Z.; Penev, E. S.; Yakobson, B. I. Two-Dimensional Mono-Elemental Semiconductor with Electronically Inactive Defects: The Case of Phosphorus. *Nano Lett.* **2014**, doi:10.1021/nl5021393.
 16. See the Supporting Information for the electronic band structure of the phosphorene allotropes discussed in Figs. 1 and 2 and the phonon band structure of θ -P.
 17. Artacho, E.; Anglada, E.; Dieguez, O.; Gale, J. D.; Garcia, A.; Junquera, J.; Martin, R. M.; Ordejon, P.; Pruneda, J. M.; Sanchez-Portal, D. *et al.* The SIESTA Method; Developments and Applicability. *J. Phys. Cond. Mat.* **2008**, *20*, 064208.
 18. Perdew, J. P.; Burke, K.; Ernzerhof, M. Generalized Gradient Approximation Made Simple. *Phys. Rev. Lett.* **1996**, *77*, 3865–3868.
 19. Tran, V.; Soklaski, R.; Liang, Y.; Yang, L. Layer-Controlled Band Gap and Anisotropic Excitons in Few-Layer Black Phosphorus. *Phys. Rev. B* **2014**, *89*, 235319.
 20. Han, X.; Stewart, H. M.; Shevlin, S. A.; Catlow, C. R. A.; Guo, Z. X. Strain and Orientation Modulated Bandgaps and Effective Masses of Phosphorene Nanoribbons. *Nano Lett.* **2014**, *14*, 4607–4614.
 21. Troullier, N.; Martins, J. L. Efficient Pseudopotentials for Plane-Wave Calculations. *Phys. Rev. B* **1991**, *43*, 1993.
 22. Ceperley, D. M.; Alder, B. J. Ground State of the Electron Gas by a Stochastic Method. *Phys. Rev. Lett.* **1980**, *45*, 566–569.
 23. Perdew, J. P.; Zunger, A. Self-interaction correction to density-functional approximations for many-electron systems. *Phys. Rev. B* **1981**, *23*, 5048–5079.
 24. Monkhorst, H. J.; Pack, J. D. Special Points for Brillouin-Zone Integrations. *Phys. Rev. B* **1976**, *13*, 5188–5192.
 25. Hestenes, M. R.; Stiefel, E. Methods of Conjugate Gradients for Solving Linear Systems. *J. Res. Natl. Bur. Stand.* **1952**, *49*, 409–436.